Supplemental Material for "Waveguide QED with Dissipative Light-Matter Couplings"

Xing-Liang Dong,[1,2] Peng-Bo Li,[1] Zongping Gong,[3,2] and Franco Nori[2,4,5]

[1] *Ministry of Education Key Laboratory for Nonequilibrium Synthesis and Modulation of Condensed Matter, Shaanxi Province Key Laboratory of Quantum Information and Quantum Optoelectronic Devices, School of Physics, Xi'an Jiaotong University, Xi'an 710049, China*

[2] *Theoretical Quantum Physics Laboratory, Cluster for Pioneering Research, RIKEN, Wakoshi, Saitama 351-0198, Japan*

[3] *Department of Applied Physics, The University of Tokyo, 7-3-1 Hongo, Bunkyo-ku, Tokyo 113-8656, Japan*

[4] *Center for Quantum Computing, RIKEN, Wakoshi, Saitama 351-0198, Japan*

[5] *Physics Department, The University of Michigan, Ann Arbor, Michigan 48109-1040, USA*

(Dated: January 13, 2025)

In this Supplemental Material, we first provide a brief review of non-Hermitian symmetries and nonunitary dynamics. We then establish a method for constructing pseudo-Hermitian Hamiltonians and demonstrate that bound states in the broken phase have equal weights across two subsystems. We prensent details about quantum emitters (QEs) in the tight-binding chain, including qualitatively different two-emitter dynamics under varying coupling strengths and a single emitter in the double-excitation sector. Additionally, we investigate the creation of third-order exceptional points (EPs) and degenerate second-order EPs using vacancy-like dressed states within simplified models. We also analyze the conditions for two-emitter bound states and show switchable light-mediated interactions in the topological lattice. Finally, we discuss the experimental feasibility of the pseudo-Hermitian waveguide QED system. We provide a method for observing level attraction through transmission spectra, propose experimental implementations using superconducting circuits, give a detailed derivation of dissipative light-matter coupling, and discuss quantum trajectories and post-selection.

SYMMETRIES AND NONUNITARY DYNAMICS IN NON-HERMITIAN SYSTEMS

In this section, we provide a concise overview of symmetries unique to non-Hermitian systems, along with the nonunitary dynamics governed by non-Hermitian Hamiltonians. The most notable are PT-symmetric systems, characterized by the commutation relation $[\hat{H}, \hat{P}\hat{T}] = 0$, where $\hat{P}$ is the parity operator and $\hat{T}$ is the time-reversal operator (antiunitary). The simplest Hamiltonian describing such a system is given by

$$\hat{H}_{PT} = \begin{pmatrix} \omega_0 + i\gamma & g \\ g & \omega_0 - i\gamma \end{pmatrix}, \tag{S1}$$

where $\hat{P} = \hat{\sigma}_x$ and there is a balance between gain and loss. The eigenvalues are either real or complex conjugate. In early experimental implementations [1–3], however, this strict requirement $\{+\gamma, -\gamma\}$ is often substituted with passive PT systems that only involve loss $\{-\gamma_1, -\gamma_2\}$. These are equivalent apart from a global exponential decay.

On the other hand, dissipative coupling is commonly linked to anti-PT symmetry, where the Hamiltonian and $\hat{P}\hat{T}$ have an anticommutative relationship $\{\hat{H}, \hat{P}\hat{T}\} = 0$. The Hamiltonian can be represented as

$$\hat{H}_{APT} = \begin{pmatrix} \omega_0 - i\gamma & -i\gamma \\ -i\gamma & -\omega_0 - i\gamma \end{pmatrix}, \tag{S2}$$

with either purely imaginary or complex eigenvalues $[E, -E^*]$. When choosing $\omega_0 = 0$, two eigenstates describe superradiance and subradiance [see Fig. S1]. Clearly, the system is purely dissipative. Inspired by passive PT systems, we can apply a purely imaginary diagonal shift to the Hamiltonian. This results in a different type of symmetry, known as pseudo-Hermitian symmetry, $\hat{\eta}^{-1}\hat{H}_{pH}\hat{\eta} = \hat{H}_{pH}^{\dagger}$, with $\hat{H}_{pH} = \hat{H}_{APT} + i\gamma\hat{I}$ and $\hat{\eta} = \hat{\sigma}_z$. More importantly, this symmetry remains valid when shifting the real energy by any amount.

Dynamical evolution governed by non-Hermitian Hamiltonians is nonunitary, for example, represented as $e^{-i\hat{H}_{APT}t}|\psi_0\rangle$. The uniform loss $-i\gamma\hat{I}$ leads to an exponential energy decay over time, $e^{-\gamma t}$. Typically, by using post-selection to select trajectories where no quantum jumps occur, trace conservation can be retrieved. Therefore, if the quantum

jump terms are omitted from the quantum master equation, a nonlinear term

$$2\gamma \mathrm{Tr}[\sum_{i,j} \hat{L}_i \hat{\rho} \hat{L}_j^\dagger]\hat{\rho} = 2\gamma \mathrm{Tr}[\sum_{i,j} \hat{\rho} \hat{L}_j^\dagger \hat{L}_i]\hat{\rho} = 2i\mathrm{Tr}[\hat{\rho}(\hat{H}_{APT} - \omega_0 \hat{\sigma}_z)]\hat{\rho} \tag{S3}$$

must be included to ensure $\mathrm{Tr}(\hat{\rho}) = 1$. At this point, the formal solution satisfies [4]

$$\hat{\rho}_t = \frac{e^{-i\hat{H}_{APT}t}\hat{\rho}_0 e^{i\hat{H}_{APT}^\dagger t}}{\mathrm{Tr}(e^{-i\hat{H}_{APT}t}\hat{\rho}_0 e^{i\hat{H}_{APT}^\dagger t})} = \frac{e^{-i\hat{H}_{pH}t}\hat{\rho}_0 e^{i\hat{H}_{pH}^\dagger t}}{\mathrm{Tr}(e^{-i\hat{H}_{pH}t}\hat{\rho}_0 e^{i\hat{H}_{pH}^\dagger t})}, \tag{S4}$$

which is one of the reasons for ignoring individual decay in the main text.

PSEUDO-HERMITIAN HAMILTONIAN FROM DISSIPATIVE COUPLINGS

We consider two arbitrary Hermitian subsystems with Hamiltonians $\boldsymbol{H}_a^{(M\times M)} = \boldsymbol{H}_a^\dagger$ and $\boldsymbol{H}_b^{(N\times N)} = \boldsymbol{H}_b^\dagger$, which are dissipatively coupled with the help of a series of auxiliary modes. In terms of block matrices, the total non-Hermitian (NH) Hamiltonian in the single-excitation sector is thus

$$\boldsymbol{H} = \boldsymbol{H}_{\mathrm{eff}} - i\kappa \boldsymbol{I} = \begin{pmatrix} \boldsymbol{H}_a & -i\boldsymbol{\kappa} \\ -i\boldsymbol{\kappa}^\dagger & \boldsymbol{H}_b \end{pmatrix} + \begin{pmatrix} -i\kappa \boldsymbol{I} & 0 \\ 0 & -i\kappa \boldsymbol{I} \end{pmatrix}, \tag{S5}$$

where $\boldsymbol{\kappa}$ denotes the coupling matrix, and the effective Hamiltonian $\boldsymbol{H}_{\mathrm{eff}}$ is pseudo-Hermitian, satisfying

$$\boldsymbol{\eta} \boldsymbol{H}_{\mathrm{eff}} \boldsymbol{\eta}^{-1} = \boldsymbol{H}_{\mathrm{eff}}^\dagger, \quad \boldsymbol{\eta} = \begin{pmatrix} \boldsymbol{I}^{(M\times M)} & 0 \\ 0 & -\boldsymbol{I}^{(N\times N)} \end{pmatrix}. \tag{S6}$$

Therefore, the eigenvalues of the effective Hamiltonian are either real or complex-conjugate pairs. Note that, as discussed with passive PT symmetry, the dynamics of the total Hamiltonian may be equivalent to the effective one, apart from a global exponential decay. When choosing two cavities as the subsystems, we obtain an anti-PT-symmetric system upon a shift of real energy. In the main text, we choose quantum emitters (QEs) and Hermitian structured waveguides as the subsystems.

This also suggests some possible directions for follow-up studies. One may study the effect of QEs dissipatively coupled to structured baths with other engineered dispersions or in higher dimension. Another idea is to construct (disordered) pseudo-Hermitian lattice models with a NH band structure, which can host different unconventional singularities, e.g., bound states in the continuum (BIC) and exceptional points (EPs). In addition, the generalization to the giant atoms case could be of interest.

BOUND STATES IN THE BROKEN PHASE

In the two-mode (two-spin) model, the dissipative coupling can generate steady Bell-like state in the PT broken phase [5, 6]. While in our work, we find $|c_e|^2 \equiv 1/2$ ($\sum_m |c_m|^2 \equiv 1/2$) when the pseudo-Hermitian symmetry is broken in the single-QE (multi-QE) case. Here, we try to derive this conclusion in a generic way. To this end, we solve the stationary Schrödinger equation

$$\boldsymbol{H}_{\mathrm{eff}} \boldsymbol{\psi} = E_B \boldsymbol{\psi}, \quad \boldsymbol{\psi} = \begin{pmatrix} \boldsymbol{C}_a \\ \boldsymbol{C}_b \end{pmatrix}, \tag{S7}$$

with eigenvalues E_B and corresponding wavefunctions $\boldsymbol{C}_a$ and $\boldsymbol{C}_b$ in subsystems a and b. For the entire system in the broken phase, there exists at least a pair of non-real eigenvalues $\{E_B, E_B^*\}$. More conjugate pairs are possible. They are unique bound states (BSs) outside the real axis. Then, we can obtain the following expressions

$$\boldsymbol{C}_a^\dagger [E_B^* \boldsymbol{I}_a - \boldsymbol{H}_a + \boldsymbol{\kappa}(E_B^* \boldsymbol{I}_b - \boldsymbol{H}_b)^{-1} \boldsymbol{\kappa}^\dagger] \boldsymbol{C}_a = 0, \tag{S8}$$

with unit matrices $\boldsymbol{I}_a = \boldsymbol{I}^{(M\times M)}$ and $\boldsymbol{I}_b = \boldsymbol{I}^{(N\times N)}$. Subtracting the two equations arrives at

$$(E_B - E_B^*) \boldsymbol{C}_a^\dagger [\boldsymbol{I}_a - \boldsymbol{\kappa} |E_B \boldsymbol{I}_b - \boldsymbol{H}_b|^{-2} \boldsymbol{\kappa}^\dagger] \boldsymbol{C}_a = 0. \tag{S9}$$

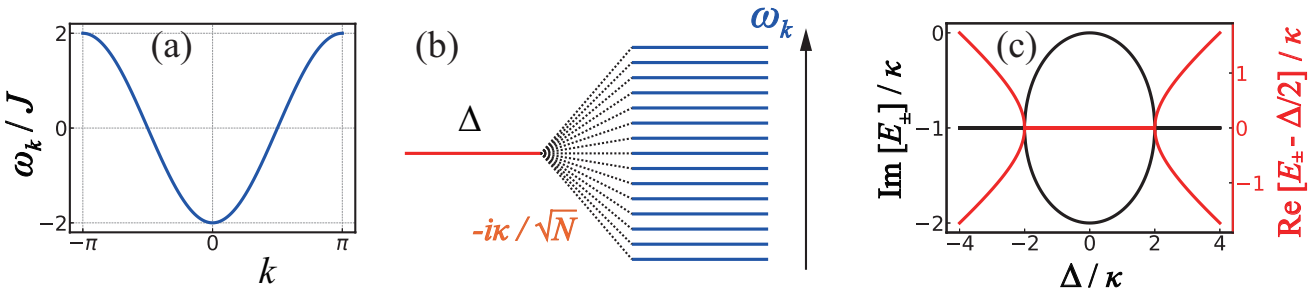

FIG. S1. (a) Energy band for the tight-binding chain, with dispersion relation $\omega_k = -2J\cos k$. (b) Single quantum emitters dissipatively coupled to a series of k modes. (c) For a single mode ($J = 0$), anti-PT symmetry can be restored by shifting the real energy by $\Delta/2$. The eigenvalues are purely imaginary in the anti-PT broken phase. However, when $J \neq 0$, the required real energy shifts vary between modes, preventing anti-PT symmetry across the spectrum. To solve this problem, we introduce pseudo-Hermitian symmetry by shifting a uniform imaginary energy of $-i\kappa$.

Because $E_B \neq E_B^*$, the rest is zero. Also, from the normalization condition $\boldsymbol{C}_a^\dagger \boldsymbol{C}_a + \boldsymbol{C}_b^\dagger \boldsymbol{C}_b = 1$, we have

$$\boldsymbol{C}_a^\dagger [\boldsymbol{I}_a + \boldsymbol{\kappa}|E_B \boldsymbol{I}_b - \boldsymbol{H}_b|^{-2} \boldsymbol{\kappa}^\dagger] \boldsymbol{C}_a = 1. \tag{S10}$$

By combining Eq. (S9) and Eq. (S10), one can deduce the final result

$$(E_B - E_B^*)(1 - 2\boldsymbol{C}_a^\dagger \boldsymbol{C}_a) = 0, \tag{S11}$$

that is $\boldsymbol{C}_a^\dagger \boldsymbol{C}_a = \boldsymbol{C}_b^\dagger \boldsymbol{C}_b = 1/2$.

EMITTERS IN THE TIGHT-BINDING CHAIN

Eigenstates of the single-emitter bound states

We consider a single emitter dissipatively coupled to the n_0th site of the coupled-resonator waveguide. As discussed in the main text, the bound states are obtained by solving the Schrödinger equation $\hat{H}_{\text{eff}}|\psi\rangle = E_b|\psi\rangle$. The eigenvalues are given by the pole equation $E_b = \Delta + \Sigma_e(E_b)$ and the photonic part of the eigenstates are calculated by

$$c_n = \frac{1}{2\pi} \int_{-\pi}^{\pi} dk e^{ikn} c_k = (ic_e/\kappa)\Sigma_e(E_b) y_{\text{min}}^{|n|}, \tag{S12}$$

where y_{min} denotes the minimum of $y_\pm$ with respect to the absolute values $|y_\pm|$, and

$$y_\pm = \frac{(-E_b \pm \sqrt{E_b^2 - 4J^2})}{2J}. \tag{S13}$$

When integrating Eq. [S12], we implemented the variable substitution $y \equiv e^{ik}$. Accordingly, $|y_\pm| \simeq 1$ represents a propagating mode without damping, while $|y_\pm| < 1$ corresponds to an exponentially localized mode. Interestingly, $y_\pm$ are purely real in the unbroken phase and complex-valued in the broken phase, which leads to a phase transition in the localization length. The atomic weight $|c_e|^2$ is obtained from the normalization condition. The localization length of the bound state is expressed as

$$\lambda = -1/\text{In}|y_{\text{min}}|. \tag{S14}$$

In the limit $\kappa \gg J$, the cavities (except for the one where the emitter is located) are completely decoupled and

$$E_\pm \simeq (\Delta \pm \sqrt{\Delta^2 - 4\kappa^2})/2. \tag{S15}$$

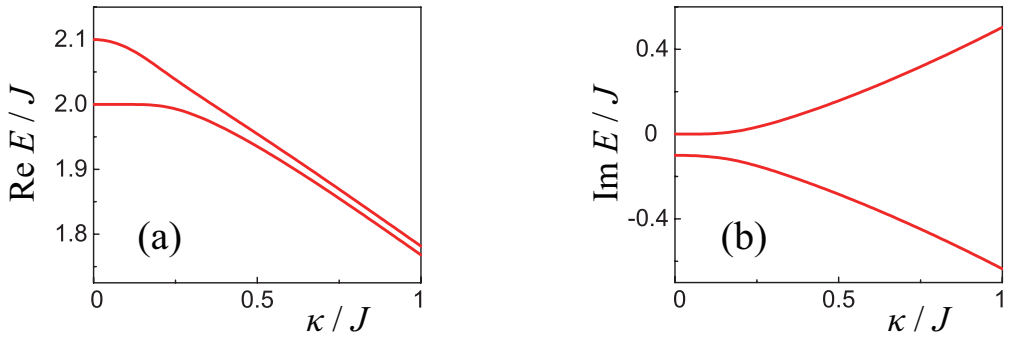

FIG. S2. Complex spectrum of the bound states with a single emitter coupled to the waveguide, and $\Delta = (2.1 - 0.1i)J$.

Pseudo-Hermitian waveguide QED

As discussed in the main text, anti-PT symmetry cannot be directly extended to continuum, because the required real energy shifts vary between modes. The uniform loss across all sites of the resonator chain is needed to achieve a consistent transformation for all k modes. In other words, the Hamiltonian can satisfy pseudo-Hermitian symmetry after an imaginary energy shift. We have figured out an intuitive physical picture by considering quantum emitter dissipatively coupled to a series of k modes [see Fig. S1]. Based on this physical picture, the following general conclusions could be intuitively understood. (i) Band regime: interaction with resonant mode $\omega_k = \Delta$ breaks pseudo-Hermitian symmetry as long as $\kappa \neq 0$, leading to localization of the resonance mode. (ii) Bandgap regime: when the coupling is sufficiently weak $\kappa \ll [\Delta - \max(\omega_k)]$, interaction with band-edge modes preserves pseudo-Hermitian symmetry, resulting in level attraction between the bound states. This physical picture may also help to clarify two other universal findings. (i) The bound states in the broken phase satisfy $(E_b - E_b^*)(2 - |c_e|^{-2}) = 0$, aligning with Bell-like states in anti-PT systems [5]. (ii) The bound state $[E_b, E_b^*]$ with a larger imaginary part dominates the long-time dynamics, reminiscent of subradiance in anti-PT systems.

In this sense, dissipative coupling and individual dissipation do not need to be equal. However, the emitter dissipation must match the cavity dissipation. To understand more clearly how the results would change if these parameters are different, we can consider the simplest scenario where the emitter has a residual imaginary energy, represented as $\Delta = \Delta_0 - i\kappa_0$. Figure S2 illustrates the bound states under these conditions. The residual imaginary energy disrupts the pseudo-Hermitian symmetry, causing the exceptional point to vanish. Nevertheless, the level attraction between the bound states persists.

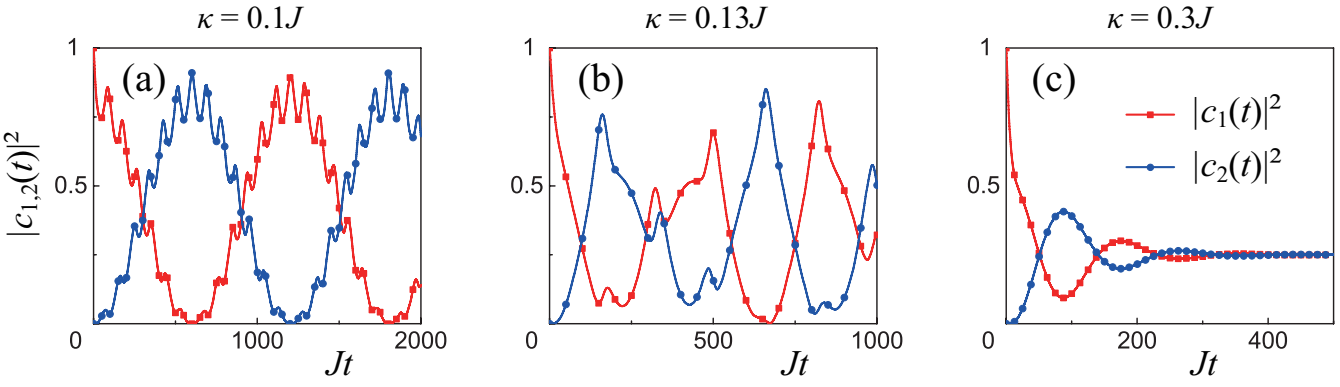

FIG. S3. Two-emitter dynamics in the bandgap regime under different coupling strengths, with $n_{12} = 7$ and $\Delta = 2.1J$. The red (blue) curve refers to the population dynamics of the initially excited (unexcited) emitter. The entire system is in the (a,b) unbroken and (c) broken phases.

Some details of the two-emitter dynamics

We consider two emitters dissipatively coupled to the n_1th and n_2th sites of the coupled-resonator waveguide. In the broken phase, the long-time dynamics is dominated by the bound states with eigenenergy of maximal imaginary parts. For simplicity, we assume that the coupling strength is large enough to have two pairs of complex-conjugate solutions $E_b = E_{\pm,p}$ $(p = s, a)$. Note that only the bound states with eigenvalues having positive imaginary parts $E_b = E_{+,p}$ may contribute to the long-time dynamics. The two-emitter bound states can still be solved from the Schrödinger equation and the pole equations are given by

$$E_b - \Delta - \Sigma_{\pm}(E_b) = 0, \quad \Sigma_{\pm}(E) = -\frac{\kappa^2}{N}\sum_k \frac{1 \pm e^{ikn_{12}}}{E - \omega_k}, \tag{S16}$$

corresponding to symmetric and antisymmetric combinations $\hat{\sigma}_{s,a} = (\hat{\sigma}_1 \pm \hat{\sigma}_2)/\sqrt{2}$, respectively. In terms of the bound states $|\psi_{\rm BS}\rangle$ and scattering eigenstates $|\psi_{\rm SE}\rangle$, the global wave function at any time reads

$$|\psi(t)\rangle \;=\; \sum_{i=1}^{4} c^i_{\rm BS}(t)|\psi^i_{\rm BS}\rangle + \sum_j c^j_{\rm SE}(t)|\psi^j_{\rm SE}\rangle, \tag{S17}$$

where $c^i_{\rm BS}(t)$ and $c^j_{\rm SE}(t)$ are the corresponding probability amplitude. For a general detuning Δ, the imaginary parts of the two eigenvalues are not equal, ${\rm Im}E_{+,s} \neq {\rm Im}E_{+,p}$, resulting in the formation of a steady state (i.e., the bound state with maximal imaginary part). It takes the general form

$$\lim_{t\to\infty}|\psi(t)\rangle \to |\psi^p_{\rm BS}\rangle = \frac{1}{2}\Big[\hat{\sigma}^\dagger_1 \pm \hat{\sigma}^\dagger_2 + (i/\kappa)\Sigma_e(E_b) \times \sum_n \big(y_{\rm min}^{|n-n_1|} \pm y_{\rm min}^{|n-n_2|}\big)\hat{a}^\dagger_n\Big]|gg\rangle|0\rangle, \tag{S18}$$

where $\pm$ is $+$ for $p = s$ and $-$ for $p = a$, depending on the separation n_{12}. Note that the existence of two bound states with unequal positive imaginary part may give rise to oscillatory damping in the excited-state population dynamics [see Fig. S3(c)].

In the main text, we discuss the special zero-detuning case ($\Delta = 0$) and show its projection towards the bound state with eigenenergy of maximal imaginary part (inter-emitter excitation oscillations) for an even (odd) emitter separation n_{12}, where $|c_1(t)|^2 + |c_2(t)|^2 = 1/2$. Here, $|c_m(t)|^2 = \langle\psi(t)|\hat{\sigma}^\dagger_m\hat{\sigma}_m|\psi(t)\rangle$ represents the population of the excited state of the quantum emitter m. This even-odd effect can be explained by Eq. (S16), which is closely related to the wave vector of the bare resonance photon. When $\Delta = 0$, the wave vector is $k = \pm\pi/2$ and the interference term is $1\pm\exp[ikn_{12}] = 1\pm1$ $(1\pm i)$ for even (odd) n_{12}. In fact, for n_{12} being an even number, one of the complex-conjugate pairs reduces to a zero-energy solution, i.e., a bound state in the continuum in the Hermitian case [7–9]. For an odd n_{12}, $E_{+,s} = -E^*_{+,a}$, thus both bound states are reserved in the long-time limit. The time evolution of the wave function can be rewritten as

$$\lim_{t\to\infty}|\psi(t)\rangle \to e^{-iE_{+,s}t}|\psi^s_{\rm BS}\rangle + e^{-iE_{+,a}t}|\psi^a_{\rm BS}\rangle. \tag{S19}$$

By examining Eq. (S18) and (S19), it becomes apparent that half of the population oscillates between the two quantum emitters, i.e., $|c_1(t)|^2 = 1/2\cos^2[{\rm Re}(E_{+,s})t]$ and $|c_2(t)|^2 = 1/2\sin^2[{\rm Re}(E_{+,s})t]$. We also point out that when the imaginary parts of the two bound states are similar, significant oscillatory behavior can be observed.

This resembles the photon-mediated collective interactions in an array of emitters in the vacuum with emitter spacing $d = n\lambda_0/4$. We note that such an effect is also applicable to the broken phase of topological waveguide QED. In the unbroken phase, the bound states have purely real eigenenergies, which lead to Hermitian-like excitation oscillation between the two emitters. Thus, in the bandgap regime, we can observe either undamped (Hermitian-like) or damped oscillations by changing the dissipative couplings, as shown in Fig. S3. The dynamics is not quite standard near the EPs.

One-emitter-per-resonator case at zero detuning $\Delta = 0$

When each resonator has a quantum emitter, two hybridized energy bands are formed. The zero-detuning ($\Delta = 0$) Bloch Hamiltonian is expressed as

$$h_k = \begin{pmatrix} 0 & -i\kappa \\ -i\kappa & -2J\cos k \end{pmatrix}. \tag{S20}$$

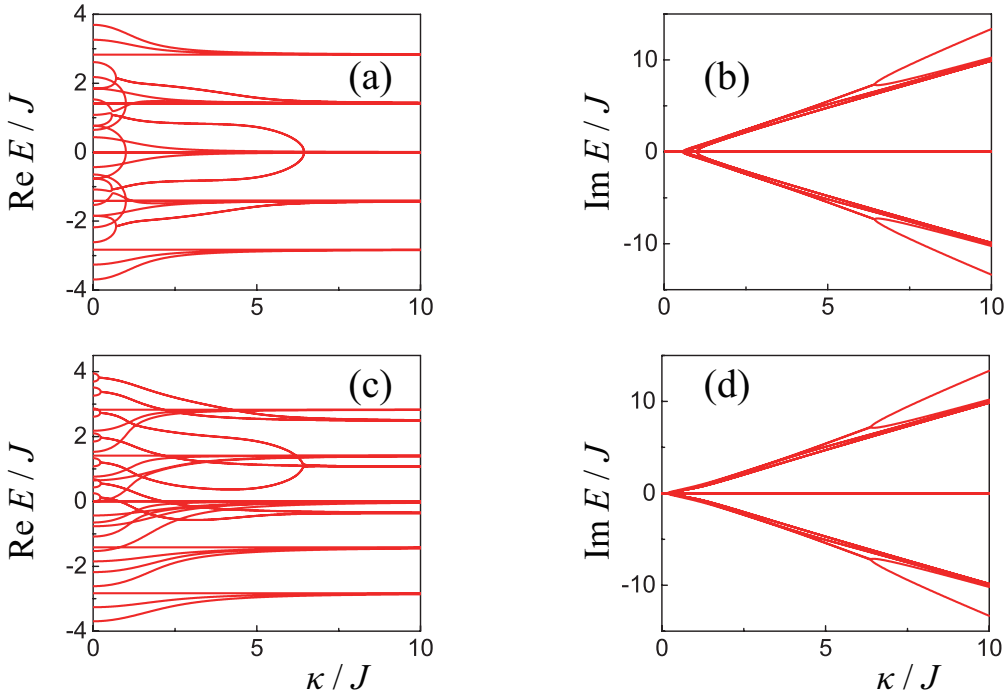

FIG. S4. Complex energy spectrum of a single emitter in the double-excitation sector, (a,b) with $\Delta = 0$, (c,d) with $\Delta = 2.1J$. Here, the number of the resonators $N = 7$.

By solving the eigen-equation, we can obtain the dispersion relation

$$\lambda_{\pm} = -J\cos k \pm \sqrt{J^2\cos^2 k - \kappa^2}, \tag{S21}$$

with corresponding eigenfunctions

$$\chi_{+} = \begin{pmatrix} -\cos\frac{\phi}{2} \\ \sin\frac{\phi}{2} \end{pmatrix}, \quad \chi_{-} = \begin{pmatrix} \sin\frac{\phi}{2} \\ \cos\frac{\phi}{2} \end{pmatrix}. \tag{S22}$$

Here, $\tan\phi = i\kappa/(J\cos k)$, and ϕ is a complex number. The k modes are real-eigenvalued (complex-conjugate) for $\kappa < J\cos k$ ($\kappa > J\cos k$). In particular, when $\kappa = J$, all bulk modes enter into the broken phase and the dissipation bands read $\mathrm{Im}\lambda_{\pm} = \mp J\sin k$. Taking the background loss into account, the zero-energy bulk modes are always the BIC, around which the dissipative band edge has a divergent density of states. For a given mode, the weights on the emitters and the resonators depend on the modulus of $\tan(\phi/2)$ [see Eq. (S22)]. In terms of the trigonometric transformation formula $\tan(\phi/2) = (-1 \pm \sqrt{1+\tan^2\phi})/\tan\phi$, we can once again show that the hybridized modes in the broken phase ($\kappa > J\cos k$) have equal weights on the emitters and the resonators (i.e., $|\tan(\phi/2)| = 1$).

A single emitter in the double-excitation sector

In the main text, we primarily consider the single-excitation scenario to initially demonstrate that when extended to continuous modes, the anti-PT symmetry linked to dissipative coupling needs to be replaced by pseudo-Hermitian symmetry. We further analyze how non-Hermitian phenomena, such as phase transitions at exceptional points, affect waveguide continuum-specific features like band structures, bound states, and spatial localization properties. In some sense, limiting the analysis to single excitations is not essential, as in the double-excitation space of a single emitter, the system can further be divided into two subspaces based on whether the atom is in the ground or excited state

$$|\psi_2\rangle = \sum_k f_1(k)\hat{a}_k^{\dagger}|e,0\rangle + \sum_{k_1,k_2} f_2(k_1,k_2)\hat{a}_{k_1}^{\dagger}\hat{a}_{k_2}^{\dagger}|g,0\rangle. \tag{S23}$$

For the Hamiltonian with dissipative light-matter couplings, the interaction between these two subspaces can be purely dissipative. Therefore, the system's Hamiltonian will naturally satisfy the pseudo-Hermitian symmetry described in Eq. [S6], leading to non-Hermitian phenomena. The same analysis applies to higher excitation numbers. Note that, as the number of excitations increases, quantum many-body challenges emerge [10], necessitating a variational approach.

Based on previous studies in conventional waveguide QED, the double-excitation states include: (i) two single-photon scattering eigenstates; (ii) one single-photon bound state and one single-photon scattering eigenstate; (iii) two-photon bound states. We expect the emergence of multiple exceptional points that correspond to the merging of bound states in the single-excitation case, as well as distinct phenomena that could arise from two-photon bound states. To verify it, we carry out a numerical study with a single emitter coupled to $N = 7$ cavities. Figure S4(a, b) depict the scenario with $\Delta = 0$, while Fig. S4(c, d) show the spectra with $\Delta = 2.1J$. We find that, beyond the emergence of multiple exceptional points, a unique behaviour emerges around $\kappa \sim 6J$, likely due to the presence of two-photon bound states. We plan to further discuss the multi-excitation scenario in our next study.

In the context of using bosonic modes as emitters in a waveguide QED setup, the system behaves linearly without limited to just one excitation. Even in the worst cases, we could observe interesting non-Hermitian phenomena at the classical level.

EMITTERS IN THE SSH LATTICE

Single-emitter bound states in the middle bandgap

We now discuss the SSH waveguide, where a single emitter is dissipatively coupled to sublattice A at the j_0th unit cell. We follow the same procedure and study the effective NH Hamiltonian, with $\hat{H}_B$ replaced by $\hat{H}_{\rm SSH}$. The single-QE self-energy becomes

$$\Sigma_{e,A}^{\rm SSH}(E) = \frac{-\kappa^2 E \,\mathrm{sign}(|y_+^{\rm SSH}| - 1)}{\sqrt{E^4 - 4J^2(1+\delta^2)E^2 + 16J^4\delta^2}}, \tag{S24}$$

where $y_\pm^{\rm SSH}$ takes the following form:

$$y_\pm^{\rm SSH} = \frac{E^2 - 2J^2(1+\delta^2) \pm \sqrt{E^4 - 4J^2(1+\delta^2)E^2 + 16J^4\delta^2}}{2J^2(1-\delta^2)}. \tag{S25}$$

For arbitrary $\Delta \in [-2J\delta, 2J\delta]$ with $\delta > 0$, the EPs in the spectrum are determined by the equations

$$\Delta = \frac{-2E_{\rm EP}^5 + 4J^2(1+\delta^2)E_{\rm EP}^3}{-E_{\rm EP}^4 + 16J^4\delta^2}, \tag{S26}$$

$$\kappa^2 = \frac{[E_{\rm EP}^4 - 4J^2(1+\delta^2)E_{\rm EP}^2 + 16J^4\delta^2]^{3/2}}{-E_{\rm EP}^4 + 16J^4\delta^2}, \tag{S27}$$

from which $E_{\rm EP} = 0$ and $\kappa = 2J\sqrt{\delta}$ for $\Delta = 0$. These two expressions give the phase diagram in the middle bandgap. The third-order EP only occurs at zero energy. Note that we can still find the localization of the resonance mode in the band regime and the pseudo-Hermitian phase transition in the upper/lower bandgap (not shown).

Enhancement of the order of the exceptional point

Previous work has demonstrated that square-root scaling of band spectra near the third-order EP is possible in the presence of sublattice symmetry [11]. In this section, we consider the simplest model consisting of a single emitter and two modes, and show that the order of the EP can be enhanced via a vacancy-like dressed state. The NH matrix is written as

$$H_3 = \begin{pmatrix} 0 & -ig & 0 \\ -ig & \Delta_1 & -t \\ 0 & -t & 0 \end{pmatrix}, \tag{S28}$$

where g denotes the dissipative coupling strength, t denotes the hopping amplitude and the detuning Δ_1 is added to break the sublattice symmetry. The three eigenvalues are $E_0 = 0$ and

$$E_\pm = \frac{\Delta_1 \pm \sqrt{\Delta_1^2 + 4t^2 - 4g^2}}{2}. \tag{S29}$$

The first eigenvalue is irrespective of the coupling strength and the associated eigenstate is $(t, 0, -ig)^T$. This refers to a vacancy-like dressed state [12]. In the case of zero detuning, there is a third-order EP at $g = t$, and the dispersion shows a square-root scaling $\sim g^{1/2}$. In the case $\Delta_1 \neq 0$ (no sublattice symmetry), the third-order EP is split into two second-order EPs. One of them corresponds to the phase transition point at $g = \sqrt{\Delta_1^2 + 4t^2}/2$. The other is still fixed at $g = t$, where a level crossing occurs. Note that such an EP is not typical because the surrounding eigenvalues are purely real.

On the other hand, a general representation of the system that exhibits an EP of order N may be obtained by a similarity transformation [13]. This representation is related to a Hatano-Nelson Hamiltonian with nonreciprocal hoppings [14]. After doing this operation, the matrix of Eq. (S28) is transformed into

$$P^{-1}H_3P = \begin{pmatrix} 0 & -t+g & 0 \\ -t-g & \sqrt{2}\Delta_1 & -t+g \\ 0 & -t-g & 0 \end{pmatrix}, \quad \text{with} \quad P = \begin{pmatrix} -\frac{\sqrt{2}}{2}i & 0 & \frac{\sqrt{2}}{2}i \\ 0 & 1 & 0 \\ \frac{\sqrt{2}}{2} & 0 & \frac{\sqrt{2}}{2} \end{pmatrix}, \tag{S30}$$

where the third-order EP arises naturally when $g = t$ and $\Delta_1 = 0$. At this point, it is a Jordan canonical form. The perturbation in $(H_3)_{i,i+1}$ corresponds to a 1-diagonal perturbation, implying that the two eigenvalues split as $E_\pm \sim g^{1/2}$ near the EP and the other one remains fixed at $E_0 = 0$.

Generation of degenerate exceptional points via vacancy-like dressed states

The minimum model for generating degenerate EPs involves two emitters and four lattice sites. Decomposed into symmetric and antisymmetric combinations, the effective NH Hamiltonian hosting degenerate EPs is expressed as

$$H_6 = H_3(\Delta_1) \oplus H_3(-\Delta_1), \tag{S31}$$

where the detuning Δ_1 comes from the hopping amplitude between the two linked lattices. Obviously, when choosing $g = t$, the eigenstate of the zero-energy solution is an arbitrary linear superposition of two orthogonal singular vectors $(1, 0, -i, 0, 0, 0)^T$ and $(0, 0, 0, 1, 0, -i)^T$. Different from initial-state independent projection $\exp\{-iH_3(\Delta_1)t\}\psi_0$ towards the singular vector $(1, 0, -i)^T$ with a global phase $\exp\{i\phi(\Delta_1)\}$, the dynamics governed by Eq. (S31) evolves towards the EPs subspace, and thus relies on the initial state. Surprisingly, we find numerically that $\exp\{i\phi(\Delta_1)\} = -\exp\{i\phi(-\Delta_1)\}$ for $\psi_0 = (0, 0, 1)^T$, which can be checked analytically by Taylor expansion.

Existence conditions of two-emitter bound states

We consider that two emitters are present. The self-energy for the symmetric and antisymmetric superposition of the two emitters $(\sigma_1 \pm \sigma_2)/\sqrt{2}$ are given by $\Sigma_\pm^{\alpha\beta} = \Sigma_e^{\text{SSH}} + \Sigma_{12}^{\alpha\beta}$, with

$$\Sigma_{12}^{AA/BB} = \frac{\kappa^2 E[y_+^{|x_{12}|}\Theta_+(y_+) - y_-^{|x_{12}|}\Theta_-(y_+)]}{\sqrt{E^4 - 4J^2(1+\delta^2)E^2 + 16J^4\delta^2}}, \tag{S32}$$

$$\Sigma_{12}^{AB} = \frac{-\kappa^2 J[F(y_+)\Theta_+(y_+) - F(y_-)\Theta_-(y_+)]}{\sqrt{E^4 - 4J^2(1+\delta^2)E^2 + 16J^4\delta^2}}, \tag{S33}$$

where $y_\pm$ are taken from Eq. (S25), $x_{12} = x_2 - x_1$ is the cell distance, $F(z) = (1+\delta)z^{|x_{12}|} + (1-\delta)z^{|x_{12}+1|}$, $\Theta_\pm(z) = \Theta(\pm 1 \mp |z|)$, and Θ is Heaviside's step function. Also, we have $\Sigma_{12}^{BA} = \Sigma_{21}^{AB}$. Then, the eigenenergy of the two-emitter bound states can be calculated by the pole equation

$$E_b - \Delta - \Sigma_\pm^{\alpha\beta}(E_b) = 0. \tag{S34}$$

However, as shown in Fig. S5, some bound states only exist after a critical coupling strength because of the cancellation of divergences at the band edges. By putting $E_b = \pm 2J\delta$ into Eq. (S34), we can obtain the critical values for the three configurations

$$\kappa_c^{\mathrm{AB}} = \sqrt{\frac{4\delta(1-\delta^2)J^2}{(2j_{12}+1)\delta - 1}}, \tag{S35}$$

$$\kappa_c^{\mathrm{BA}} = \sqrt{\frac{4\delta(1-\delta^2)J^2}{(2j_{12}-1)\delta + 1}}, \tag{S36}$$

$$\kappa_c^{\mathrm{AA/BB}} = \sqrt{\frac{2(1-\delta^2)J^2}{j_{12}}}, \tag{S37}$$

where $\delta > 0$ and the denominators under the square root need to be positive values.

Two-QE dynamics in the topological waveguide

Typically, chiral BSs can mediate chiral interactions, depending on the sublattices to which the QEs are coupled. Here, the incorporation of pseudo-Hermiticity results in unconventional behaviours. Specifically, we consider three configurations with two QEs coupled to (i) AA, (ii) AB and (iii) BA sublattices. It is worth mentioning that the emitter spacing is even (odd) for the first case AA (the latter two cases, AB and BA). We plot both the real part of the energy spectrum and the QEs dynamics in Fig. S5. For the AB configuration, we show a perfect coherent transfer of half of the excitation between the two QEs, see Fig. S5(e). The zero-energy solutions vanish and the oscillation frequency reaches the maximum at the spectral singularities, as shown in Fig. S5(b).

The sublattice symmetry is unbroken in the symmetric/antisymmetric subspace for the AA configuration, which is evidenced by the existence of 3rd order EPs [see Fig. S5(a)]. The phase transition dependent on dissipative

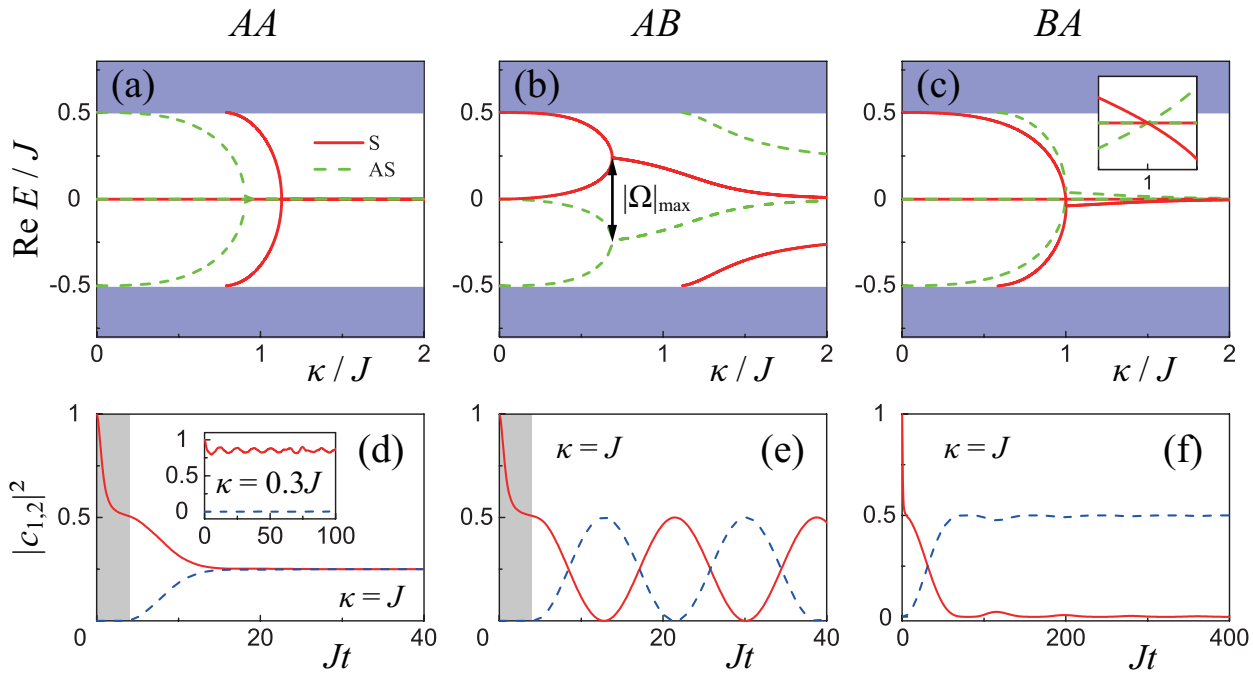

FIG. S5. Emitters in a topological waveguide. Here, $\Delta = 0$ and $\delta = 0.25$. (a,b,c) Real part of the energy eigenvalues and (d,e,f) population dynamics of two QEs. In the two-QE spectra, the solid red (dash green) lines represent the BSs of symmetric (antisymmetric) combination. (a,d) AA configuration with unit cell spacing $j_{12} = 3$; (b,e) AB configuration with $j_{12} = 3$; (c,f) BA configuration with $j_{12} = 4$.

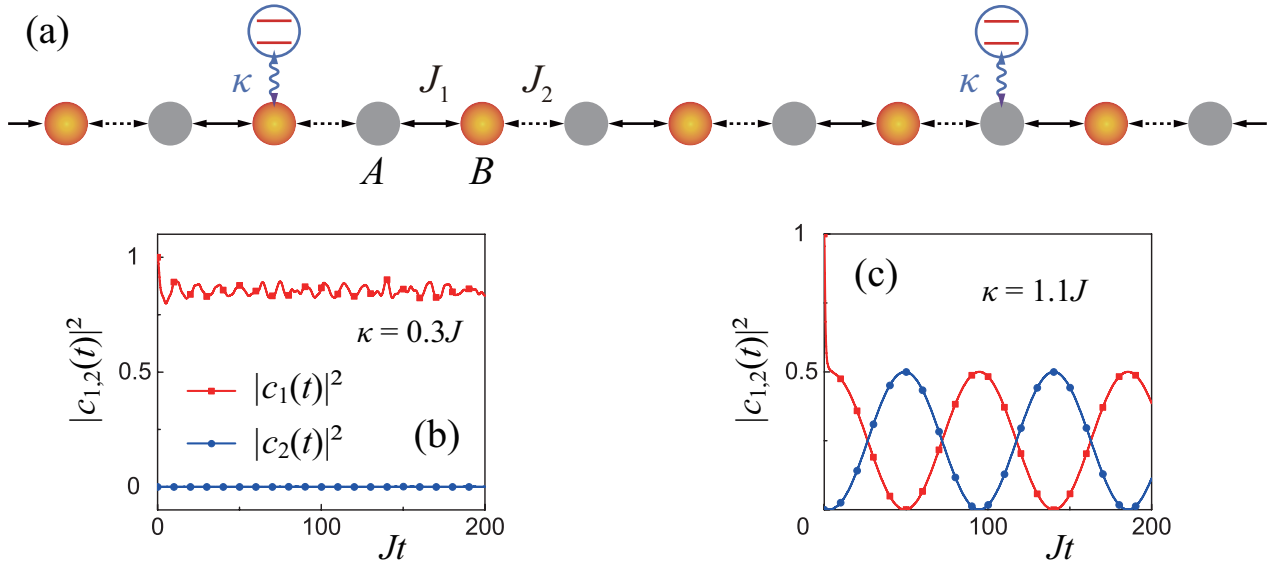

FIG. S6. (a) Two emitters dissipatively coupled to a topological SSH waveguide at different locations, with cell separation $j_{12} = 4$. Here, A/B labels the sublattice, κ is the dissipative coupling, $J_1 = J(1+\delta)$ is the intracell hopping and $J_2 = J(1-\delta)$ is the intercell hopping, with $\delta = 0.25$. Corresponding population dynamics with (b) $\kappa = 0.3J$ and (c) $\kappa = 1.1J$, respectively. The red (blue) curve refers to the population dynamics of the initially excited (unexcited) emitter.

couplings allows for switchable dipole-dipole interaction, as shown in Fig. S5(d). That is, with (without) light-mediated interaction in the broken (unbroken) phase. The BA configuration also allows switchable interaction between the two QEs. In Fig. S6, we plot the two-QE dynamics with the same parameters, except for taking different coupling strengths. When $\kappa = 0.3J$, the interaction is prohibited. When $\kappa = 1.1J$, we show a perfect coherent transfer of half of the excitation between the two QEs. This is a little different from the case of the AB configuration, where the bound state with eigenenergy of maximal imaginary part is reserved in the long-time limit. Actually, it is closely related to the even-odd effect discussed before.

The dynamics is much more peculiar for the BA configuration, as shown in Fig. S5(f). When the initially excited emitter is coupled to the A (B) sublattice, the final state is $|\psi_{\rm vds}^{j_1,B}\rangle$ ($|\psi_{\rm vds}^{j_2,A}\rangle$). More generally, the final state will be a linear superposition of two singular vectors $|\psi_f\rangle \propto \cos\alpha|\psi_{\rm vds}^{j_2,A}\rangle + e^{i\beta}\sin\alpha|\psi_{\rm vds}^{j_1,B}\rangle$, for an arbitrary initial state except for an eigenstate. According to the energy spectrum, we find an accidental degeneracy of two 2nd order EPs at zero energy [see inset in Fig. S5(c)], which is responsible for the initial-state dependent projection. This is consistent with the situation previously discussed in the simplified model. These spectral degeneracies, known as diabolically degenerate exceptional points, have exhibited the ability to control mode switching [15–17].

EXPERIMENTAL FEASIBILITY

Detailed derivation of dissipative couplings

To obtain the required effective NH coupling between a two-level system and a single-mode cavity, one can couple both of them to an auxiliary cavity mode or the traveling waves. For the auxiliary cavity realization, the light-matter coupling is obtained to be

$$g_{\rm eff} \simeq \frac{-ig_\sigma g_a}{\kappa_{\rm aux} - i\Delta_c}, \tag{S38}$$

which is inevitably accompanied by a coherent interaction [18, 19]. Here, g_σ (g_a) and Δ_c are the coupling and detuning between the emitter (mode $\hat{a}$) and the auxiliary cavity, and $\kappa_{\rm aux}$ denotes the decay rate of the auxiliary mode. A nearly pure dissipative coupling $-ig_\sigma g_a/\kappa_{\rm aux}$ is possible only in the limit of large dissipation $\kappa_{\rm aux} \gg \Delta_c$. In contrast, the traveling-wave realization can induce purely dissipative interaction and thus may be preferable. In this case, an emitter and a photonic mode are coupled with identical strength $g_\sigma = g_a$ to a common Markovian bath at a distance

$x_{a\sigma} = x_a - x_\sigma$. The Hamiltonian in the interaction picture is expressed as

$$\hat{H}_{SR}(t) = \frac{g_a}{\sqrt{L}}\Big\{\hat{a}^\dagger \sum_q e^{i[(\omega_a-\omega_q)t-qx_a]}\hat{r}_q + \hat{\sigma}^\dagger \sum_q e^{i[(\omega_\sigma-\omega_q)t-qx_\sigma]}\hat{r}_q\Big\} + \text{H.c.}, \tag{S39}$$

where L is the length of the waveguide, $\hat{r}_q$ and $\omega_q = cq$ are the annihilation operator and angular frequency of the photon with wave vector q. Within the Born-Markov approximation, the reduced density operator of the system obeys the following equation [20]

$$\dot{\hat{\rho}}_S = -\int_0^t dt' \ \text{Tr}_R\big\{[\hat{H}_{SR}(t), [\hat{H}_{SR}(t'), \hat{\rho}_S(t)\hat{R}_0]]\big\}. \tag{S40}$$

Here, we assume the initial reservoir $\hat{R}_0$ being in the vacuum with $\langle \hat{r}_q^\dagger \hat{r}_q\rangle = 0$ and consider that the emitter is nearly resonant with the cavity mode $\omega_\sigma \approx \omega_a$. After adiabatically eliminating the reservoir degrees of freedom, we obtain the standard Lindblad master equation

$$\dot{\hat{\rho}}_S = 2\kappa\big(\mathcal{D}[\hat{a}] + \mathcal{D}[\hat{\sigma}]\big)\hat{\rho}_S + 2\kappa_{a\sigma}\big(\mathcal{D}[\hat{a},\hat{\sigma}] + \mathcal{D}[\hat{\sigma},\hat{a}]\big)\hat{\rho}_S, \tag{S41}$$

with Lindbald superoperator $\mathcal{D}[\hat{L}_1,\hat{L}_2]\hat{\rho} \equiv \hat{L}_1\rho\hat{L}_2^\dagger - \{\hat{L}_1^\dagger\hat{L}_2/2, \hat{\rho}\}$, collective damping rate $\kappa_{a\sigma} = \kappa e^{iq(\omega_a)|x_{a\sigma}|}$ and $\kappa = c^{-1}g_a^2$. When the separation satisfies $q(\omega_a)|x_{a\sigma}| = 2\pi n$, with n being the integer, we arrive at the dissipative interaction term without redundant coherent interaction [21, 22]. However, in addition to the dissipative coupling, there appear undesired local losses which are very detrimental to observing bound states. To circumvent these, we should couple the remaining lattice sites to individual dissipation channels to achieve uniform on-site damping at a rate of κ.

Transmission spectrum as an observable

A possible alternative to observing level attraction and singularity is based on the coupled anti-resonances. We first revisit the coupled anti-resonances in anti-PT symmetric systems [23], calculating the transmission coefficient using the input-output relations. We then extend this to scenarios involving multiple photon modes. For simplicity, we assume bosonic modes as emitters. Given that mode $\hat{a}$ (photon) and $\hat{b}$ (emitter) each possess an intrinsic damping rate α and are dissipatively coupled via the waveguide mode, the Hamiltonian can be formulated as:

$$\hat{H}_1 = [\omega_b - i(\alpha+\gamma)]\hat{b}^\dagger\hat{b} + [\omega_a - i(\alpha + \frac{\kappa^2}{\gamma})]\hat{a}^\dagger\hat{a} - i\kappa(\hat{a}^\dagger\hat{b} + \text{H.c.}). \tag{S42}$$

Here, γ and κ^2/γ denote the dissipation of modes $\hat{a}$ and $\hat{b}$ into the waveguide, respectively, while κ represents the strength of the dissipative coupling. We consider the right-going traveling photons. Assuming $\gamma \gg \{\alpha,\kappa\} \gg \kappa^2/\gamma$, and applying the Heisenberg equation of motion in the steady-state ($\dot{\hat{a}} = 0$, $\dot{\hat{b}} = 0$), we can derive the two coupled equations as follows

$$[i(\omega-\omega_b) - (\alpha+\gamma)]\hat{b} - \kappa\hat{a} - i\sqrt{\gamma}\hat{p}_{in} = 0, \tag{S43}$$

$$i(\omega-\omega_a)\hat{a} - \alpha\hat{a} - \kappa\hat{b} = 0, \tag{S44}$$

where we drop the input term and the dissipation term related to κ^2/γ. By considering the input-output relation $\hat{p}_{in} = \hat{p}_{out} + i\sqrt{\gamma}\hat{b}$, we can get

$$S(\omega) = \frac{\hat{p}_{out}}{\hat{p}_{in}} = 1 + \frac{\gamma}{i(\omega-\omega_b) - (\alpha+\gamma) - \frac{\kappa^2}{i(\omega-\omega_a)-\alpha}}, \tag{S45}$$

which determines the full transmission coefficient of two coupled anti-resonances. This can be seen from the inversed transmission coefficient

$$\frac{1}{S(\omega)} = 1 - \frac{\gamma}{i(\omega-\omega_b) - \alpha - \frac{\kappa^2}{i(\omega-\omega_a)-\alpha}}, \tag{S46}$$

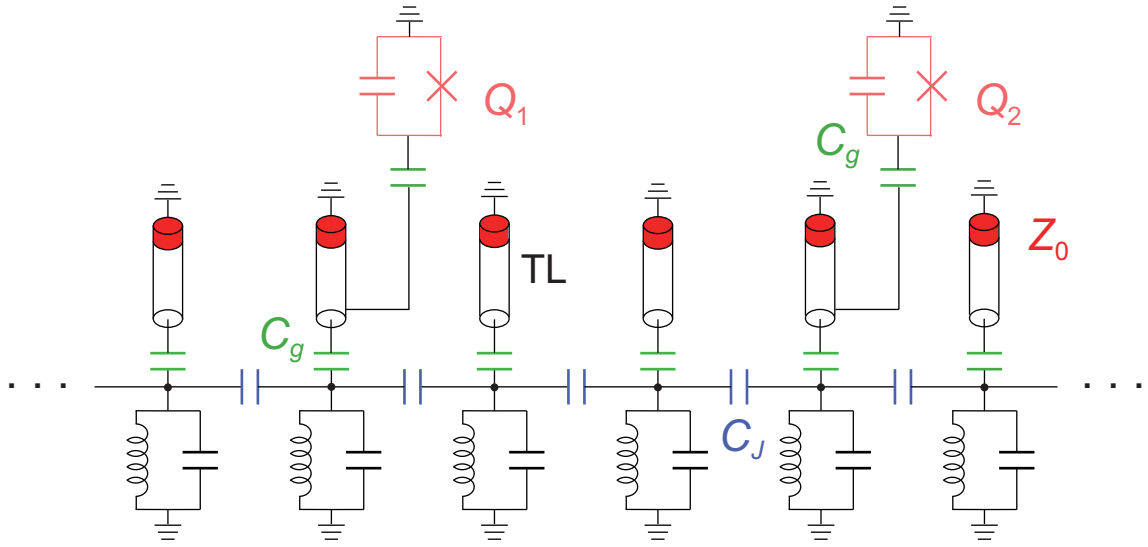

FIG. S7. Schematic electrical circuits for physically implementing the proposed pseudo-Hermitian waveguide QED systems. The adjacent LC resonators are capacitively coupled to realize the structured waveguide. To generate on-site dissipation, each LC resonator is capacitively coupled to a Markovian transmission line (TL), which is terminated with resistive elements to ensure genuine dissipation. The transmon qubits corresponding to the QEs are capacitively coupled to the TLs to realize dissipative light-matter couplings.

with the denominator corresponding to the characteristic polynomial of matrix

$$H = \begin{pmatrix} \omega_b & -i\kappa \\ -i\kappa & \omega_a \end{pmatrix} - i\alpha I. \tag{S47}$$

This means we can extract eigenvalues of an anti-PT symmetric system through transmission spectrum.

To extend to multiple photon modes or even continuous modes, we need to rewrite the coupled equations as

$$[i(\omega-\omega_b)-(\alpha+\gamma)]\hat{b} - \frac{\kappa}{\sqrt{N}}\sum_k \hat{a}_k - i\sqrt{\gamma}\hat{p}_{in} = 0, \tag{S48}$$

$$i(\omega-\omega_k)\hat{a}_k - \alpha\hat{a}_k - \frac{\kappa}{\sqrt{N}}\hat{b} = 0, \quad k=1,2,\ldots,N. \tag{S49}$$

Again, we assume $\gamma \gg \{\alpha,\kappa\} \gg \kappa^2/\gamma$ and drop the terms related to κ^2/γ. One can easily arrive at the inversed transmission coefficient for a series of k modes

$$\frac{1}{S(\omega)} = 1 - \frac{\gamma}{i(\omega-\omega_b)-\alpha-\frac{1}{N}\sum_{k=1}^{N}\frac{\kappa^2}{i(\omega-\omega_k)-\alpha}}, \tag{S50}$$

with the denominator corresponding to the characteristic polynomial of matrix

$$H = \frac{1}{\sqrt{N}}\begin{pmatrix} \Delta\sqrt{N} & -i\kappa & -i\kappa & \cdots & -i\kappa \\ -i\kappa & \omega_1\sqrt{N} & 0 & \cdots & 0 \\ -i\kappa & 0 & \omega_2\sqrt{N} & \cdots & 0 \\ \vdots & \vdots & \vdots & \ddots & \vdots \\ -i\kappa & 0 & 0 & \cdots & \omega_N\sqrt{N} \end{pmatrix} - i\alpha I_{N+1}. \tag{S51}$$

In general, inspired by the anti-PT symmetric system, we find in principle that extending this approach to continuous modes may keep the transmission spectrum as a useful observable. It is worth mentioning that by revisiting pseudo-anti-PT symmetric systems, the quantum squeezing dynamics could be a possible physical observable [24], where the dynamical stability of Hermitian systems is related to the non-Hermitian matrix. We plan to address this possibility further in our subsequent work.

Possible implementation in circuit QED platforms

The master equation in Eq. (1) of the main text may be physically implemented with superconducting circuits that have demonstrated the ability to explore conventional waveguide QED. Building upon previous experiments [25, 26], we propose a feasible circuit scheme to realize dissipative couplings between the QEs and the waveguide, as shown in Fig. S7. To convert to a topological waveguide, the uniform capacitors C_J need to be replaced with alternate capacitors C_{J_1} and C_{J_2}.

Estimation of the number of trajectories for post-selection

In our work, the quantum jump terms in the master equation are replaced by a nonlinear term that is added to ensure $\mathrm{Tr}(\hat{\rho}) = 1$. This is justified by appropriate post-selections in the experiment [27–31]. There are several ways to achieve this, such as building a larger Hermitian system using auxiliary modes and then measuring those modes, continuously monitoring the environment in real time, or tracking the system's dynamics.

In superconducting circuit experiments [32–34], post-selection can be performed by first reconstructing the complete density matrix of the quantum state using quantum state tomography. This involves conducting a series of projection measurements to collect data on the system's projections in different bases. Using these data, the density matrix can be reconstructed. During data processing, only the matrix elements within the n-excitation sector (for instance, the single-excitation sector) are retained, while all other elements are set to zero. The resulting density matrix is then renormalized. This process ensures that only the relevant quantum states are considered for analysis.

In our pseudo-Hermitian waveguide QED systems, the timescale of non-Hermitian dynamical process is about an order of magnitude larger than the excitation lifetime κ^{-1}. This means the dynamical signal of concern will dissipate rapidly when taking quantum jumps into account. Therefore, a significant challenge for observing dissipative dynamics is that many trajectories may be needed to make post-selection, so that there is at least one without quantum jumps. The jump probability within a short time interval is given by $P_{\mathrm{jump}}(t) \sim \kappa \delta t$. By choosing $\delta t \ll \kappa^{-1}$, the number of trajectories can be simply estimated as $\sim 10^4$. Finally, we mention that the novel non-Hermitian phenomena discussed in the single-excitation sector could also be observed at the classical level.

[1] A. Guo, G. J. Salamo, D. Duchesne, R. Morandotti, M. Volatier-Ravat, V. Aimez, G. A. Siviloglou, and D. N. Christodoulides, Observation of $\mathcal{PT}$-symmetry breaking in complex optical potentials, Phys. Rev. Lett. **103**, 093902 (2009).

[2] S. Bittner, B. Dietz, U. Günther, H. L. Harney, M. Miski-Oglu, A. Richter, and F. Schäfer, $\mathcal{PT}$ Symmetry and Spontaneous Symmetry Breaking in a Microwave Billiard, Phys. Rev. Lett. **108**, 024101 (2012).

[3] B. Peng, Ş. K. Özdemir, S. Rotter, H. Yilmaz, M. Liertzer, F. Monifi, C. M. Bender, F. Nori, and L. Yang, Loss-induced suppression and revival of lasing, Science **346**, 328 (2014).

[4] D. C. Brody and E.-M. Graefe, Mixed-State Evolution in the Presence of Gain and Loss, Phys. Rev. Lett. **109**, 230405 (2012).

[5] H. Y. Yuan, P. Yan, S. Zheng, Q. Y. He, K. Xia, and M.-H. Yung, Steady Bell State Generation via Magnon-Photon Coupling, Phys. Rev. Lett. **124**, 053602 (2020).

[6] J. Zou, S. Zhang, and Y. Tserkovnyak, Bell-state generation for spin qubits via dissipative coupling, Phys. Rev. B **106**, L180406 (2022).

[7] L. Zhou, H. Dong, Y.-x. Liu, C. P. Sun, and F. Nori, Quantum supercavity with atomic mirrors, Phys. Rev. A **78**, 063827 (2008).

[8] C. W. Hsu, B. Zhen, A. D. Stone, J. D. Joannopoulos, and M. Soljačić, Bound states in the continuum, Nat. Rev. Mater. **1**, 16048 (2016).

[9] M. Mirhosseini, E. Kim, X. Zhang, A. Sipahigil, P. B. Dieterle, A. J. Keller, A. Asenjo-Garcia, D. E. Chang, and O. Painter, Cavity quantum electrodynamics with atom-like mirrors, Nature **569**, 692 (2019).

[10] T. Shi, Y.-H. Wu, A. González-Tudela, and J. I. Cirac, Bound States in Boson Impurity Models, Phys. Rev. X **6**, 021027 (2016).

[11] I. Mandal and E. J. Bergholtz, Symmetry and Higher-Order Exceptional Points, Phys. Rev. Lett. **127**, 186601 (2021).

[12] L. Leonforte, A. Carollo, and F. Ciccarello, Vacancy-like Dressed States in Topological Waveguide QED, Phys. Rev. Lett. **126**, 063601 (2021).

[13] Y.-X. Xiao, J. Hu, Z.-Q. Zhang, and C. T. Chan, Experimental demonstration of splitting rules for exceptional points and their topological characterization, Phys. Rev. B **108**, 115427 (2023).

[14] N. Hatano and D. R. Nelson, Localization Transitions in Non-Hermitian Quantum Mechanics, Phys. Rev. Lett. **77**, 570 (1996).

[15] R. Melanathuru, S. Malzard, and E.-M. Graefe, Landau-Zener transitions through a pair of higher-order exceptional points, Phys. Rev. A **106**, 012208 (2022).

[16] I. I. Arkhipov *et al.*, Dynamically crossing diabolic points while encircling exceptional curves: A programmable symmetric-asymmetric multimode switch, Nat. Commun. **14**, 2076 (2023).

[17] I. I. Arkhipov *et al.*, Fully solvable finite simplex lattices with open boundaries in arbitrary dimensions, Phys. Rev. Res. **5**, 043092 (2023).

[18] Y.-P. Wang and C.-M. Hu, Dissipative couplings in cavity magnonics, J. Appl.Phys. **127**, 130901 (2020).

[19] Y. Zhang, W. Nie, and Y.-x. Liu, Edge-State Oscillations in a One-Dimensional Topological Chain with Dissipative Couplings, Phys. Rev. Appl. **18**, 024038 (2022).

[20] H.-P. Breuer and F. Petruccione, *The theory of open quantum systems* (Oxford University Press on Demand, 2002).

[21] Y.-F. Qiao, H.-Z. Li, X.-L. Dong, J.-Q. Chen, Y. Zhou, and P.-B. Li, Phononic-waveguide-assisted steady-state entanglement of silicon-vacancy centers, Phys. Rev. A **101**, 042313 (2020).

[22] W. Nie, M. Antezza, Y.-x. Liu, and F. Nori, Dissipative Topological Phase Transition with Strong System-Environment Coupling, Phys. Rev. Lett. **127**, 250402 (2021).

[23] Y. Yang, Y.-P. Wang, J. W. Rao, Y. S. Gui, B. M. Yao, W. Lu, and C.-M. Hu, Unconventional Singularity in Anti-Parity-Time Symmetric Cavity Magnonics, Phys. Rev. Lett. **125**, 147202 (2020).

[24] X.-W. Luo, C. Zhang, and S. Du, Quantum Squeezing and Sensing with Pseudo-Anti-Parity-Time Symmetry, Phys. Rev. Lett. **128**, 173602 (2022).

[25] E. Kim, X. Zhang, V. S. Ferreira, J. Banker, J. K. Iverson, A. Sipahigil, M. Bello, A. González-Tudela, M. Mirhosseini, and O. Painter, Quantum Electrodynamics in a Topological Waveguide, Phys. Rev. X **11**, 011015 (2021).

[26] X. Zhang, E. Kim, D. K. Mark, S. Choi, and O. Painter, A superconducting quantum simulator based on a photonic-bandgap metamaterial, Science **379**, 278 (2023).

[27] U. Günther and B. F. Samsonov, Naimark-Dilated $\mathcal{PT}$-Symmetric Brachistochrone, Phys. Rev. Lett. **101**, 230404 (2008).

[28] Y. Wu, W. Liu, J. Geng, X. Song, X. Ye, C.-K. Duan, X. Rong, and J. Du, Observation of parity-time symmetry breaking in a single-spin system, Science **364**, 878 (2019).

[29] W. Tang, X. Jiang, K. Ding, Y.-X. Xiao, Z.-Q. Zhang, C. T. Chan, and G. Ma, Exceptional nexus with a hybrid topological invariant, Science **370**, 1077 (2020).

[30] L. Xiao, K. Wang, X. Zhan, Z. Bian, K. Kawabata, M. Ueda, W. Yi, and P. Xue, Observation of Critical Phenomena in Parity-Time-Symmetric Quantum Dynamics, Phys. Rev. Lett. **123**, 230401 (2019).

[31] R. Shen, T. Chen, M. M. Aliyu, F. Qin, Y. Zhong, H. Loh, and C. H. Lee, Proposal for Observing Yang-Lee Criticality in Rydberg Atomic Arrays, Phys. Rev. Lett. **131**, 080403 (2023).

[32] K. W. Murch, S. Weber, C. Macklin, and I. Siddiqi, Observing single quantum trajectories of a superconducting quantum bit, Nature **502**, 211 (2013).

[33] M. Naghiloo, M. Abbasi, Y. N. Joglekar, and K. W. Murch, Quantum state tomography across the exceptional point in a single dissipative qubit, Nat. Phys. **15**, 1232 (2019).

[34] P.-R. Han, F. Wu, X.-J. Huang, H.-Z. Wu, C.-L. Zou, W. Yi, M. Zhang, H. Li, K. Xu, D. Zheng, H. Fan, J. Wen, Z.-B. Yang, and S.-B. Zheng, Exceptional Entanglement Phenomena: Non-Hermiticity Meeting Nonclassicality, Phys. Rev. Lett. **131**, 260201 (2023).